

# Multiple steady states in a radio frequency chlorine glow discharge

Eray S. Aydil and Demetre J. Economou<sup>a)</sup>

Department of Chemical Engineering, University of Houston, Houston, Texas 77204-4792

(Received 4 June 1990; accepted for publication 10 September 1990)

Multiple steady states have been observed in a 13.56 MHz chlorine glow discharge in a parallel plate radial flow reactor. Measurements of the flux and energy distribution of positive ions bombarding the electrode are reported along with radial profiles of atomic chlorine (Cl) concentration and etch rate of polysilicon for different states of the plasma. At the same operating conditions the plasma may exist in one of two states. In one state the plasma appeared radially uniform, resulting in relatively uniform radial Cl concentration profiles and etch rate. In the other state the plasma appeared radially nonuniform with a higher intensity central region ("plasmoid"). The etch rate and Cl concentration profiles were nonuniform in the presence of the plasmoid. The plasmoid generally appeared under conditions of high power and pressure and could be eliminated by adding noble gases and/or decreasing the electrode spacing. The multiple states may be a result of the strongly electronegative nature of the chlorine discharge.

## I. INTRODUCTION

Plasma etching using low-pressure reactive gas discharges (glow discharges) has become the dominant technique in the microelectronics industry for delineating fine patterns in thin solid films.<sup>1</sup> Reactive gas plasmas are also employed for the deposition of thin films. A common reactor configuration is that of a parallel plate (diode) etcher, in which the discharge is created between two parallel electrodes with the wafer(s) resting on one of the electrodes.

Plasma etching with chlorine or chlorinated gases is used extensively for the etching of silicon, aluminum, and compound semiconductors.<sup>2</sup> A number of experimental and theoretical investigations of the chlorine discharge have been reported.<sup>3-8</sup> Close examination of the reported studies reveals that the chlorine plasma is a source of unusual phenomena, perhaps due to the electronegative nature of the plasma. For example, a large concentration of negative ions ( $\text{Cl}^-$ ),<sup>7</sup> and anomalous optogalvanic signals of  $\text{Cl}^-$  have been reported near the sheath. These phenomena may be due to the formation of double layers between the plasma and the electrodes, a result of high negative ion density compared to the electron density.<sup>8</sup>

Multiple states in gas discharges have been reported and studied before, especially for dc discharges. Dettmer<sup>9</sup> (see also references therein) observed two steady states in the positive column of a dc discharge in oxygen. However, reports of multiple states in rf discharges of the kind used for electronic materials processing are scarce. Lamont and DeLeone<sup>10</sup> reported the formation of "plasmoids" in an argon discharge used for sputtering. Sawin<sup>4</sup> studied rf chlorine discharges, and mentioned that different steady states accompanied by hysteresis and instabilities were observed. Flamm *et al.*<sup>11</sup> observed different "modes" in a  $\text{CF}_3\text{Br}$  discharge and studied their effect on deposition and etching qualitatively. Despite the fact that multiple states have

been observed in reactive gas plasmas, the authors are not aware of any quantitative studies of such multiple states and their possible consequences on the etching or deposition process.

## II. EXPERIMENT

Experiments were performed in a parallel plate single wafer reactor. The 8-in. diam showerhead aluminum upper electrode had a heavy anodization layer and was held at an adjustable distance from the equal area stainless-steel (SS) lower electrode. Unless noted otherwise, the interelectrode spacing was 1 in. The upper electrode was powered by a 500 W, 13.56 MHz generator. Gas pressure and flow rate(s) were controlled independently using closed loop control systems. Gases used were ultrapure chlorine and prepurified argon, the latter used as actinometer. The temperature of both electrodes was controlled by a chiller/heater. Unless noted otherwise, a temperature of 293 K was used. The plasma chamber communicated with a differentially pumped analysis chamber through a 100- $\mu$  pinhole in the SS lower electrode. The pressure in the analysis chamber was kept at approximately  $10^{-6}$  Torr using a turbomolecular pump. For etching experiments, the lower electrode was replaced by another SS electrode which had a groove cut in the center to accommodate a 100-mm silicon wafer, such that the wafer surface was flush with the electrode surface. The details of the experimental system and the plasma diagnostics will be described in a future publication.

The flux and energy distribution of positive ions bombarding the electrode were measured by a Faraday cup/retarding grid analyzer.<sup>12</sup> The main ion bombarding the electrode is expected to be  $\text{Cl}_2^+$ . Optical emission actinometry was used to monitor the radial atomic chlorine concentration profiles. The experimental arrangement for the

<sup>a)</sup> Author to whom correspondence should be addressed.

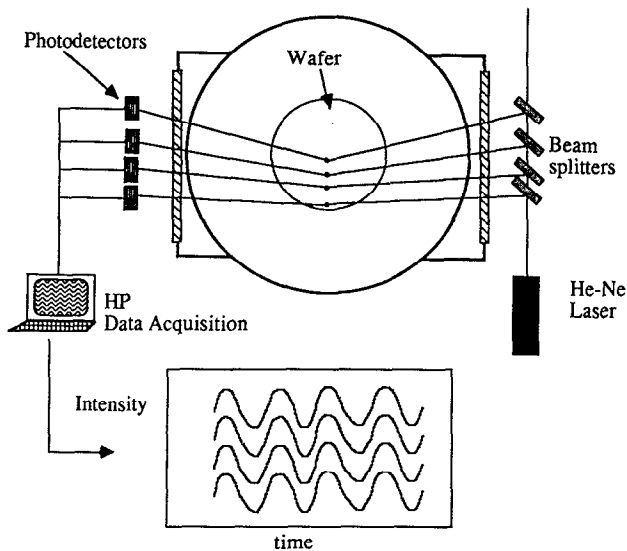


FIG. 1. Schematic of the spatially resolved laser interferometry apparatus.

optical emission diagnostics has been described by Economou *et al.*<sup>13</sup> Briefly, the plasma emission was collected through a set of pinholes to attain spatial resolution. The light was focused onto an optical fiber and was transmitted to a monochromator. The dispersed light was detected using a diode-array detector. The 837.6-nm Cl atom line and the 811.5-nm Ar line were used for actinometry. Data were processed as before<sup>13</sup> in order to obtain the Cl atom radial concentration profiles.

There is some controversy regarding the application of actinometry to monitor Cl atoms in a chlorine discharge<sup>5,14</sup> as the discharge parameters vary. Actinometry can be used to monitor the Cl atom density when the excited state, whose emission is being monitored, is created by electron impact excitation only. The relative contribution of other mechanisms producing the excited state must be negligible. Reactions such as dissociative excitation and dissociative attachment may produce excited chlorine atoms and thus make actinometry invalid. Gottscho and Donnelly<sup>14</sup> concluded from observations of the spectral line shapes that actinometry is invalid for Cl atoms if the emission from the sheaths is sampled. However, it was found that the 837.6-nm line can be used to monitor the Cl atom concentration actinometrically if emission is sampled from the plasma center. Richards *et al.*<sup>5</sup> found actinometry to be invalid for monitoring Cl atoms. However, the authors sampled the emission from the entire discharge, including the sheaths. In the present work, optical emission from the central plane of the discharge away from the sheaths was sampled.

The etch rate of polysilicon was measured *in situ* using spatially resolved laser interferometry (Fig. 1). This technique is an extension of conventional laser interferometry,<sup>15,16</sup> and uses multiple laser beams and detectors. The beam from a He-Ne laser (632.8 nm) was split into multiple beams (four in this study) using beamsplitters, which

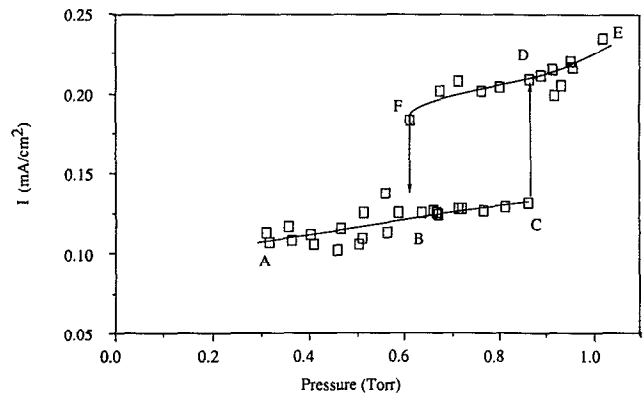


FIG. 2. Ion bombardment flux as a function of pressure. Other conditions were 100 W, 1-in. electrode spacing, and 25 sccm.

were directed to different radial positions on the wafer. The specular reflection intensity from each radial position was monitored using photodetectors. The reflected intensity varied periodically as the thickness of the film being etched changed, and the etch rate at each radial position was calculated from the period of the intensity variation. Multi-channel interferometry provided an *in situ* measurement of etch rate and uniformity.

### III. RESULTS AND DISCUSSION

Figure 2 shows the ion bombardment flux, as measured by the Faraday cup, as a function of pressure at a power of 100 W, and a flow rate of 25 sccm of pure chlorine. The ion flux versus pressure exhibits hysteresis, and two steady states are observed for identical discharge conditions. As the pressure was increased slowly, starting from 0.3 Torr, the ion flux increased slightly following branch *ABC* until point *C* was reached at a pressure of 0.86 Torr. At that point a sudden increase in the ion flux was recorded as the discharge entered the upper state. Further increase in pressure yielded trace *DE*. Conversely, as the pressure was slowly lowered starting from point *E*, the upper branch *EDF* was described down to a pressure of 0.60 Torr (point *F*), at which point the discharge returned to the lower branch. Further decrease in pressure resulted in trace *BA*. The experimental data points in Fig. 2 were collected in two experiments on different days, and the scatter of the data represents the reproducibility of the measurements.

The appearance of the discharge in the two states was distinctly different. In the lower state *ABC*, the radial distribution of the plasma glow appeared rather uniform. However, in the upper state *FDE*, the radial distribution of the plasma glow was nonuniform, having a central region of higher emission intensity, surrounded by a diffuse region extending to the electrode edges (Fig. 3). The higher intensity central region will be hereafter called the "plasmoid." During the transition from one branch to the other, the plasmoid appeared or disappeared rather suddenly. The diameter of the plasmoid was a function of the operating conditions (especially power), and it was in the range of 2–4 in. for the parameter values studied. By using a

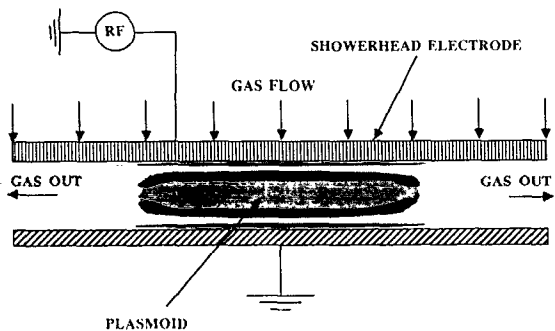


FIG. 3. Schematic drawing of the plasmoid.

sufficiently high power, the plasmoid diameter could be made equal to the electrode diameter. The *axial* distribution of the plasma glow in the plasmoid was nonuniform, with striations as shown schematically in Fig. 3.

The higher emission intensity of the plasmoid suggests that the power density is higher in the plasmoid as compared to the rest of the discharge. A higher power density implies higher rates of ionization and dissociation in the plasmoid. Hence, as soon as the plasmoid forms, the ion flux (measured through a pinhole in the electrode center) increases suddenly (transition from *C* to *D*). Conversely, as soon as the plasmoid disappears the measured ion flux decreases suddenly (transition from *F* to *B*). The critical pressure at which the plasmoid appeared (disappeared) depended on how fast the pressure was increased (decreased) as one moved along the lower (upper) branch, as well as how tightly the flow rate and incident power were controlled. In the experiments reported here, the pressure was changed in small increments, and allowed to reach a steady value. The matching network was subsequently tuned to minimize the reflected power.

Figure 4 shows the behavior of the ion bombardment flux as a function of power for a constant pressure of 0.7 Torr. Conditions were otherwise as in Fig. 2. Two hysteresis loops are observed, one at approximately 45 W and the other in the range of 70–140 W. A fully developed plasmoid was not observed in association with the low-power

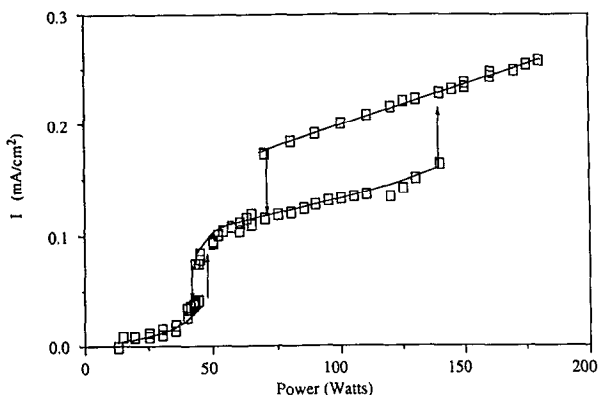


FIG. 4. Ion bombardment flux as a function of power. Other conditions were 0.7 Torr, 1-in. electrode spacing, and 25 sccm.

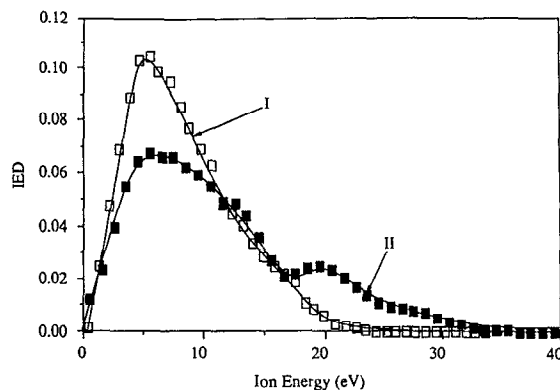


FIG. 5. Ion energy distribution functions in the absence (curve I) and in the presence (curve II) of the plasmoid. Conditions were 0.7 Torr, 100 W, 1-in. electrode spacing, and 25 sccm.

loop, although the plasma appeared somewhat more intense towards the center. However, a plasmoid was clearly formed in association with the high-power loop. In general, the ion flux increases with increasing power since the ion density in the plasma increases with power. This may also result in a thinner sheath, reducing the number of collisions the ions suffer in their transit through the sheath, thereby increasing the ion flux to the electrode.

The ion bombardment energy distribution was also affected by the presence of the plasmoid. Figure 5 shows the ion energy distribution (IED) function for identical reactor operating conditions. Both curves have been normalized such that the area under each curve is unity. Curve I corresponds to the lower branch of Fig. 2, in which a plasmoid does not form. Curve II corresponds to the upper branch of Fig. 2 in which a plasmoid forms. In the presence of a plasmoid, the IED function extends towards higher bombardment energies. This can be explained by the higher power density in the plasmoid resulting in higher voltage (and perhaps thinner) sheaths. The median ion energy versus pressure (Fig. 6) and power (Fig. 7) also exhibited hysteresis. The median ion energy is defined

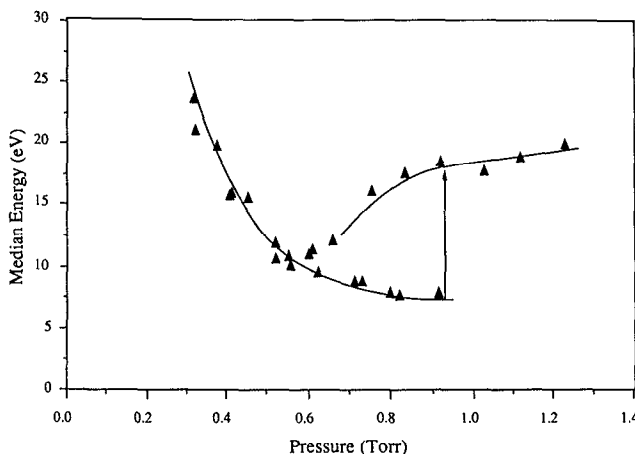


FIG. 6. Median ion bombardment energy as a function of pressure. Other conditions were 100 W, 1-in. electrode spacing, and 25 sccm.

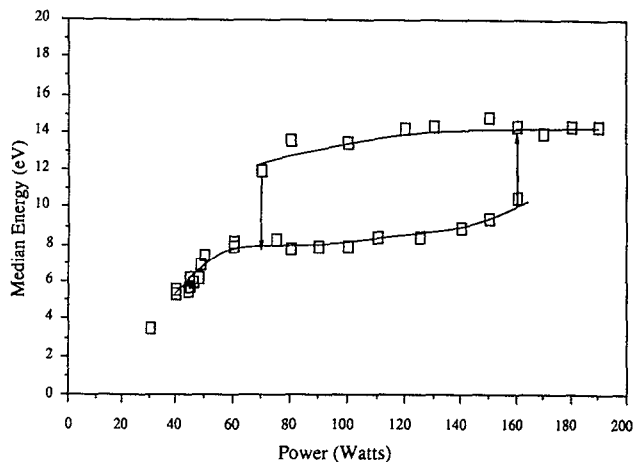


FIG. 7. Median ion bombardment energy as a function of power. Other conditions were 0.7 Torr, 1-in. electrode spacing, 25 sccm.

such that half the ions striking the electrode have energies lower than the median, and the other half have energies higher than the median. Under the present experimental conditions, the median energy is also representative of the average ion bombardment energy (the two differed by a few eV). In the presence of the plasmoid, both the ion flux to the grounded electrode and the energy of the ions were higher than in the absence of the plasmoid. The low-power loop evident in Fig. 4 is not apparent in Fig. 7 due to the experimental resolution of the median energy ( $\pm 1$  eV) and the expected inaccuracy of the energy analyzer below 5 eV. However the high-power loop associated with the plasmoid formation is clearly seen in Fig. 7.

The plasmoid could also be obtained when the stainless-steel lower electrode was replaced with an alumina electrode. In fact, a plasmoid was formed even in the presence of a silicon wafer. Figure 8 shows the radial distribution of the atomic chlorine density, as measured by actinometry, in the absence and presence of the plasmoid

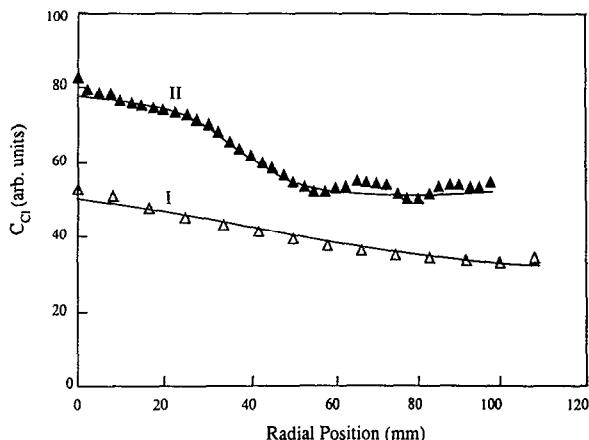


FIG. 8. Atomic chlorine radial concentration profiles in the absence (curve I, 0.5 Torr) and in the presence (curve II, 0.7 Torr) of the plasmoid during etching of polysilicon film. Other conditions were 100 W, 1-in. electrode spacing, and 25 sccm.

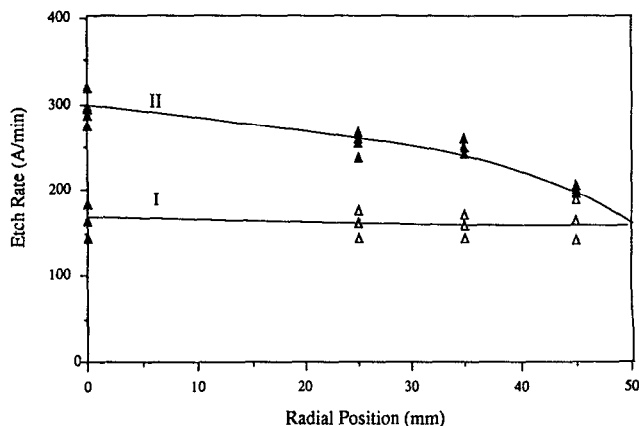


FIG. 9. Polysilicon radial etch rate profiles in the absence (curve I) and in the presence (curve II) of the plasmoid. Conditions were as in Fig. 8.

(curves I and II, respectively). A 100-mm wafer covered with a lightly P-doped polysilicon film was resting on the lower SS electrode. The power was 100 W, and the total flow rate was 25 sccm (including 5% Ar used as actinometer). At a pressure of 0.5 Torr a plasmoid is not formed (see also Fig. 2), and the Cl atom density is only slightly nonuniform over the polysilicon surface (curve I). However, the situation is considerably different at a pressure of 0.7 Torr. At this pressure, a plasmoid is formed over the wafer surface and the  $\text{Cl}_2$  dissociation rate is higher in the plasmoid (central) region due to higher power density in the plasmoid. This results in substantially larger Cl atom density gradients with the Cl atom density decreasing from the wafer center to the edge (curve II).

The polysilicon etch rate, as measured by spatially resolved multichannel interferometry, is shown in Fig. 9. Curves I and II correspond to the same conditions as curves I and II of Fig. 8. In the absence of the plasmoid the etch rate is uniform (curve I). In the presence of the plasmoid the etch rate is higher but nonuniform (curve II). The etch rate distribution does not exactly follow the Cl atom density distribution shown in Fig. 8. The etch rate of the lightly doped polysilicon is expected to have a substantial contribution from ion-assisted reactions. Hence the uniformity of the ion bombardment flux will influence the etch uniformity. Under the conditions of Figs. 8 and 9, the diameter of the plasmoid was slightly smaller than the wafer diameter. The etching nonuniformity would have been more severe if larger wafers (e.g., 200 mm) were used.

The plasmoid was not always stable. At extreme conditions (e.g., very high power and pressure), the plasmoid could become unstable, moving off center (symmetry breaking), "jumping" from place to place in a seemingly chaotic fashion, or even rotating between the electrodes.

The plasmoid generally appeared under conditions of high power and pressure. For example, for the relatively low pressure of 0.3–0.5 Torr, a plasmoid was not observed in the power range (10–180 W) examined. Also, for power values lower than 50 W, a plasmoid was not observed in the pressure range (0.1–1.0 Torr) examined. Electrode

temperature had a substantial effect. For example, when the electrodes were heated to 323 K, no hysteresis was observed in the ion flux versus pressure (0.3–1 Torr) curve for a power of 100 W (compared to Fig. 2 which is for an electrode temperature of 293 K). However, a slight hysteresis was observed in the ion flux versus power (10–180 W) curve for an electrode temperature of 323 K. The effect of electrode spacing was dramatic. No hysteresis was seen for an electrode spacing of 0.5 in. over the pressure (0.3–3.0 Torr) and power (10–180 W) ranges examined.

Instabilities and multiple steady states have often been observed in dc discharges, including stationary and traveling waves. For example, Dettmer<sup>9</sup> observed two different forms of the oxygen discharge sustained in a long tube. He also observed sharp changes in the discharge variables (such as the electric field, current, and atomic oxygen density) as the discharge shifted from one state to the other. The necessary condition for this so-called attachment-ionization instability is that the attachment rate coefficient increases faster than the ionization rate coefficient<sup>17</sup> as the electron temperature increases, i.e.,

$$\frac{\partial k_a}{\partial T_e} > \frac{\partial k_i}{\partial T_e}.$$

However, our calculations and those of others<sup>3</sup> showed that the above inequality is not satisfied for the chlorine discharge. Therefore, the present results cannot be explained by the attachment-ionization instability mechanism.

Another form of instability often observed at high-pressure high-current conditions results in a constriction of the discharge away from the walls of the confining tube.<sup>18</sup> This is attributed to radial gradients in the gas temperature. If the temperature in the central region of the discharge is higher than the edge temperature, the gas number density is lower at the center. This condition can trigger an instability whereby the lower gas number density results in higher electron temperature, and therefore higher ionization rate and current density in the center of the discharge. This in turn leads to higher temperature in the center and a feedback mechanism. The formation of the plasmoid in the experiments presented here could be thought of as a form of discharge constriction. However, the temperature gradients expected under our experimental conditions are probably too low to induce such an instability (see also Ref. 19).

Taillet<sup>20</sup> used a theory developed by Vandenplas and Gould<sup>21</sup> to show that some plasmoids observed in low pressure ( $10^{-4}$ – $10^{-1}$  Torr) rf discharges can be due to the plasma becoming resonance sustained, a series resonance between a capacitive sheath and an inductive bulk plasma. The bulk plasma impedance may have an inductive component due to the inertial mass of the electrons, when the electron collision frequency is less than the applied field frequency. The range of pressures used in this study is high enough such that the electron collision frequency is larger than the applied frequency, and bulk plasma inductance arising from electron inertia may be neglected. However, strongly electronegative plasmas with ion density much

higher than the electron density may exhibit an inductive component due to inertia of the ions.<sup>22,23</sup> In another recent study, contractions of the positive column in electronegative gases were studied theoretically.<sup>24</sup>

Experiments were conducted under conditions for which a plasmoid could be obtained by appropriate adjustment of the pressure (e.g., 100 W, 25 sccm, 1 in. spacing). Different amounts of a noble gas were added to the discharge keeping the total flow rate constant. Pressure was then increased slowly starting from 0.5 Torr. Additions of He or Ar increased the critical pressure at which the plasmoid appeared. For example, the critical pressure at which the plasmoid appeared was increased from 0.86 Torr for pure chlorine to 1.2 Torr by adding 20% He or 40% Ar to the discharge. In another set of experiments, the plasma was operated under conditions where a plasmoid was present (pure chlorine, 0.7 Torr, 100 W, 25 sccm, 1 in. spacing). Then small amounts of He or Ar were bled into the discharge. The flow rate of the additive gas was changed in small increments, and after a change in the flow rate, the discharge was allowed to relax in its steady state. The plasmoid was seen to disappear when the additive gas concentration exceeded approximately 15% for either He or Ar. Nitrogen addition had a dramatic effect. The plasmoid did not appear even when 1% nitrogen was added to the discharge.

The formation of the plasmoid and the associated instabilities and hysteresis observed in the chlorine discharge may be due to the strongly electronegative nature of the discharge. Indeed, the negative ion density in the Cl<sub>2</sub> discharge is two orders of magnitude higher than the electron density.<sup>3</sup> Addition of He or Ar may result in a lower concentration ratio of negative ions to electrons, and hence increased electropositive behavior of the plasma.

#### IV. CONCLUDING REMARKS

Besides being interesting in their own right, the hysteresis and multiple steady states have important implications from the practical point of view. For example, non-uniform etching may result in the presence of a plasmoid as demonstrated, or the plasma conditions may be irreproducible. Further, care should be exercised when trying to characterize a plasma process using empirical methods, such as response surface methodology, which assume that the dependent variables are a continuous function of the process parameters. Finally, it comes as no surprise to see that in many practical etching systems employing electronegative plasmas, He or Ar gases are added to “stabilize” and “homogenize” the plasma.

In summary, multiple steady states in a 13.56 MHz chlorine glow discharge in a single-wafer etcher have been observed. Ion bombardment flux and energy, atomic chlorine radial concentration profiles, and poly-Si etch rate profiles were presented for the different plasma states. The occurrence of instabilities and multiple steady states in the chlorine discharge may be due to the strongly electronegative nature of the discharge.

## ACKNOWLEDGMENTS

We are grateful to the National Science Foundation (CBT 8708908) and to Texas Instruments for financial support of this work. Thanks are due to Dr. Gabe Barna and Dr. Wayne Fisher of Texas Instruments for technical support.

- <sup>1</sup>D. M. Manos and D. L. Flamm, eds., *Plasma Etching: An Introduction* (Academic, New York, 1989).
- <sup>2</sup>N. G. Einspruch and D. M. Brown, eds., *VLSI Electronics: Microstructure Science, Vol. 8, Plasma Processing for VLSI* (Academic, New York, 1984).
- <sup>3</sup>G. L. Rogoff, J. M. Kramer, and R. B. Piejak, *IEEE Trans. Plasma Sci.*, **PS-14**, 103 (1986).
- <sup>4</sup>H. H. Sawin, A. D. Richards, and B. E. Thompson, *ACS Symp. Series*, **290**, 164 (1985).
- <sup>5</sup>A. D. Richards, B. E. Thompson, K. D. Allen, and H. H. Sawin, *J. Appl. Phys.* **62**, 792 (1987).
- <sup>6</sup>V. M. Donnelly, D. L. Flamm, and R. Bruce, *J. Appl. Phys.* **58**, 2135 (1985).
- <sup>7</sup>G. S. Selwyn, L. D. Baston, and H. H. Sawin, *Appl. Phys. Lett.* **51**, 898 (1987).
- <sup>8</sup>R. A. Gottscho and C. E. Gaebe, *IEEE Trans. Plasma Sci.* **PS-14**, 92 (1986).
- <sup>9</sup>J. W. Dettmer, Ph.D. thesis, Air Force Institute of Technology (1978).
- <sup>10</sup>L. T. Lamont, Jr. and J. J. DeLeone, Jr., *J. Vac. Sci. Technol.* **7**, 155 (1969).
- <sup>11</sup>D. L. Flamm, P. L. Cowan, and J. A. Golovchenko, *J. Vac. Sci. Technol.* **17**, 1341 (1980).
- <sup>12</sup>B. E. Thompson, K. D. Allen, A. D. Richards, and H. H. Sawin, *J. Appl. Phys.* **59**, 1890 (1986).
- <sup>13</sup>D. J. Economou, S.-K. Park, and G. D. Williams, *J. Electrochem. Soc.* **136**, 188 (1989).
- <sup>14</sup>R. A. Gottscho and V. M. Donnelly, *J. Appl. Phys.* **56**, 245 (1984).
- <sup>15</sup>H. H. Busta, R. E. Lajos, and D. A. Kiewit, *Solid State Technol.* **22**, 61 (1979).
- <sup>16</sup>M. Sternheim, W. van Gelder, and A. W. Hartman, *J. Electrochem. Soc.* **130**, 655 (1983).
- <sup>17</sup>R. A. Haas, *Phys. Rev. A* **8**, 1017 (1973).
- <sup>18</sup>E. F. Jaeger, L. Oster, and A. V. Phelps, *Phys. Fluids* **19**, 819 (1976).
- <sup>19</sup>D. B. Ogle and G. A. Woosley, *J. Phys. D Appl. Phys.* **20**, 453 (1987).
- <sup>20</sup>J. Taillet, *Am. J. Phys.* **37**, 423 (1969).
- <sup>21</sup>P. E. Vandenplas and R. W. Gould, *Physica*, **28**, 357 (1962).
- <sup>22</sup>E. Gogolides, J.-P. Nicolai, and H. H. Sawin, *J. Vac. Sci. Technol. A* **7**, 1001 (1989).
- <sup>23</sup>H. Shan, S. A. Self, and J. P. McVittie, 177th *Electrochem. Soc. Meeting Extended Abstracts* **90-1**, No. 103, 145 (1990).
- <sup>24</sup>P. G. Daniels, R. N. Franklin, and J. Snell, *J. Phys. D Appl. Phys.* **23**, 823 (1990).